

# Polymerisable Octahedral Rhenium Cluster Complexes as Precursors for Photo/Electroluminescent Polymers

Olga A. Efremova,<sup>a</sup> Konstantin A. Brylev,<sup>b,c</sup> Olena Kozlova,<sup>d</sup> Matthew S. , Michael A. Shestopalov,<sup>b,c</sup> Noboru Kitamura,<sup>f</sup> Yuri V.

Mironov,<sup>b,c</sup> Siegfried Bauer,<sup>d</sup> Andrew J. Sutherland<sup>\*a</sup>

<sup>a</sup> Chemical Engineering and Applied Chemistry, Aston University, Aston Triangle, Birmingham, B4 7ET, UK; Fax: +44 (0)121 204 3679; Tel: +44 (0)121 204 3425; E-mail: a.j.sutherland@aston.ac.uk

<sup>b</sup> Nikolaev Institute of Inorganic Chemistry SB RAS, 3 Acad. Lavrentiev Ave., 630090 Novosibirsk, Russia; Fax: +7(383) 330-94-89; Tel: +7(383) 330-92-53; E-mail: kbrylev@gmail.com

<sup>c</sup> Novosibirsk State University, 2 Pirogova Str., 630090 Novosibirsk, Russia

<sup>d</sup> Department of Soft Matter Physics, Johannes-Kepler University, Altenbergerstr. 69, Linz, A-4040, Austria

<sup>e</sup> Linz Institute for Organic Solar Cells (LIOS), Physical Chemistry, Johannes Kepler University, Linz 4040, Austria

<sup>f</sup> Department of Chemistry, Faculty of Science, Hokkaido University, 060-0810 Sapporo, Japan

**KEYWORDS:** Rhenium cluster complexes, Organic Polymers, Photoluminescence, Electroluminescence

New polymerisable photoluminescent octahedral rhenium cluster complexes *trans*-[ $\{ \text{Re}(\text{TBP})_4(\text{VB})_2 \}$ ] (Q = S or Se; TBP – *p*-*tert*-butylpyridine; VB – vinyl benzoate) have been synthesised, characterised and used to construct rhenium cluster-organic polymer hybrid materials. These novel polymer systems are solution-processable and the rhenium clusters retain their photoluminescent properties within the polymer environment. Notably, when the rhenium cluster complexes are incorporated into the matrix of the electroluminescent polymer poly(*N*-vinylcarbazole), the resultant cluster polymer hybrid combined properties of both components and was used successfully in the construction of a polymer light emitting diode (PLED). These prototype devices are the first PLEDs to incorporate octahedral rhenium clusters and provide the first direct evidence of the electroluminescent properties of rhenium clusters and indeed, to the best of our knowledge, of any member of the family of 24-electron hexanuclear cluster complexes of molybdenum, tungsten or rhenium.

## INTRODUCTION

Inorganic-organic hybrids based on photoluminescent octahedral clusters  $\{ \text{M}(\text{L})_6 \}$  (where M is Mo, W or Re; Q – inner ligands that are either halogens or chalcogens and L are various outer ligands) are an attractive, new class of materials.<sup>18</sup> They offer the opportunity to combine the excellent photoluminescent properties of octahedral cluster complexes (i.e. long living photoluminescence in the red/near-infrared region (NIR) with high quantum yields) with some useful properties conferred by the organic components. They may also exhibit new properties that are not found in the individual components. In general, photoluminescent metal complexes incorporated into organic polymers/macromolecules have advantages over small molecules in manufacturing light emitting/harvesting devices as they can be readily processed to coat large areas (e.g. by spin-coating, doctor blade coating or ink jet printing). Systems where the metal centres and organic components are bonded on the nanometre scale are more preferable for manufacturing purposes than simple blended systems, as they tend not to undergo phase separation.<sup>19</sup>

Several approaches have been described previously that led to the development of such hybrid materials. For example,  $\{ \text{Re}(\text{OH})_6 \}^{4+}$  anions were encapsulated directly into

maltose-decorated poly(propylene amine) dendrimers significantly increasing the hydrolytic stability of the rhenium cluster complex.<sup>20</sup> Outer ligand metathesis reaction of  $\{ \text{Re} \}^{2+}$  with promesogenic ligands was employed to generate molybdenum cluster-based liquid crystal materials.<sup>21</sup> The same approach of ligand metathesis reaction was used to develop cluster-organic polymer hybrids, i.e. highly cross-linked poly(methyl methacrylate) (PMMA) and polystyrene (PS) polymers containing clusters.<sup>22</sup> Zheng *et al.* have shown another approach to obtain cluster-organic polymer hybrids, in which cluster complexes, functionalised by ATRP-initiating ligands, were used to obtain non-cross-linked rhenium cluster-containing PMMA polymers.<sup>23</sup> Finally, in previous work we presented the  $\{ \text{Re} \}(\text{TBP})_4(\text{MAC})_2$  (TBP = *p*-*tert*-butylpyridine, MAC – methacrylate ions) cluster complex that was copolymerised with methyl methacrylate (MMA) by means of both bulk- and solution-based polymerisation.<sup>14</sup> In that work we showed that the cluster unit fully retains its intrinsic photoluminescent properties in the hybrid material, while its presence in low concentration does not significantly affect the properties (e.g. processability) of the polymer matrix. At the same time, this cluster complex showed relatively poor solubility in common organic solvents, which significantly limits its use in a solution-based

polymerisation reaction thus hindering access to materials with higher concentrations of the cluster complex.

Herein we report the synthesis and characterisation of novel, soluble, readily polymerisable octahedral cluster complexes *trans*-[ $\text{Ru}(\text{TBP})_4(\text{VB})_2$ ], where VB = vinyl benzoate and Q = S (**1**) or Se (**2**). These cluster complexes can be utilised for synthesising photoluminescent organic polymers using solution-based techniques. To exemplify the approach, we have copolymerised the new complexes with MMA, styrene and *N*-vinylcarbazole using a free radical-initiated solution-based polymerisation in chlorobenzene and evaluated the properties of the resulting copolymers. PMMA and PS were chosen as they are excellent examples of commodity polymers that are transparent in the red to NIR, have good mechanical properties, and are suitable for processing by both solution and melt-based approaches. Furthermore, poly(*N*-vinylcarbazole) (PVK)-based hybrids were examined as PVK possesses good electroluminescent properties with an emission maximum located in violet-blue region (i.e. in the region, where rhenium cluster complexes absorb well). Fluorescent dyes or phosphorescent dopants<sup>24, 25</sup> are used widely in combinations with PVK in polymer organic light-emitting diodes (PLEDs) to improve device efficiency<sup>26-29</sup> or to tune the colour.<sup>30, 31</sup> Accordingly, we have designed PLEDs employing a -PVK-based hybrid material and studied their electroluminescent properties.

## EXPERIMENTAL SECTION

### Materials

The complexes *trans*-[ $\text{Ru}(\text{TBP})_4(\text{OH})_2$ ] (Q = S or Se) were obtained according to the earlier report.<sup>32</sup> All other reactants were purchased from either Alfa Aesar or Aldrich. Styrene and methyl methacrylate were purified from inhibitors by washing with a 2M NaOH solution and drying over magnesium sulphate. AIBN and *N*-vinylcarbazole were recrystallized twice from methanol. Other reactants were used as received. Dialysis tubing (molecular weight cut-offs 3500 and 7000 D) were purchased from Medicell Ltd.

### Instrumentation

NMR spectra were recorded on a Bruker Avance 300 NMR spectrometer equipped with a solution-state dual channel probe working at 300.13 MHz for <sup>1</sup>H and 75 MHz for <sup>13</sup>C. NMR spectra were measured in CDCl<sub>3</sub> ( $\delta = 7.26$ ,  $\delta = 77.16$ ) in the standard way using the zg30 pulse program for <sup>1</sup>H and waltz16 pendant pulse program for <sup>13</sup>C. MS analyses of **1** and **2** were conducted using a WATERS Micromass LCT (ESI) mass spectrometer in methanol in the presence of NaI. Elemental analyses were obtained from EuroVector EA3000 Elemental Analyser. FTIR was recorded on a Bruker Vertex 80 as KBr disks. Absorption spectra of **1** and **2** were recorded in diapaon 270-700 nm on a PerkinElmer Lambda35 UV/Vis spectrometer. Thermal transition temperatures were determined under a nitrogen atmosphere using a Mettler Toledo DSC 1 differential scanning calorimeter. The heating and cooling rates were kept at 20 °C/min, with sample weights – 4.0-8.0 mg. Indium

was utilised as a reference for calibrating the temperature.  $T_d$  was estimated to be the midpoint temperature of the endothermic baseline shift. Polymer decomposition temperatures ( $T_d$ ) were found by thermogravimetric analysis (TGA) on a NETZSCH TG 209 F1 Iris Thermo Microbalance in a stream of helium (30 mL min<sup>-1</sup>) at a heating rate of 20 K min<sup>-1</sup> and reported as temperatures of onset of intense thermal degradation determined by the point of intersection of the tangents to two branches of the thermogravimetric curves. Polymer molecular weights ( $M_n$ ) were determined using gel permeation chromatography (GPC) using a degassed THF eluent system containing 2 % TEA and 0.05 % (w/v) BHT through three PL gel 5  $\mu\text{m}$  300 x 7.5 mm mixed C columns. The system, operating at 40 °C with an eluent flow rate of 1 mL min<sup>-1</sup>, was calibrated against narrow polystyrene standards ( $M_n$  ranged from 162 to 6 035 000 g mol<sup>-1</sup>).

### Photoluminescence Measurements

For photoluminescence measurements, powdered samples of the complexes **1** and **2** and the cluster co-polymers based on **1** and **2** were placed between two non-fluorescent glass plates. The absorbance of dichloromethane solutions of **1** and **2** was set at < 0.1 at 355 nm. The solutions were poured into quartz cuvettes. For deaeration, an Ar-gas stream was purged through the solutions for 30 min and then the cuvettes were sealed. Measurements were carried out at 298 K. The samples were excited by 355-nm laser pulses (6 ns duration, LOTIS TII, LS-2137/3). Corrected emission spectra were recorded on a red-light-sensitive multichannel photodetector (Hamamatsu Photonics, PMA-11). For emission decay measurements, the emission was analysed by a streakscope system (Hamamatsu Photonics, C4334 and C5094). The emission quantum yields ( $\Phi$ ) for the solutions were estimated by using [Ru(bpy)<sub>3</sub>](ClO<sub>4</sub>)<sub>2</sub> as a standard:  $\Phi = 0.095$  in deaerated acetonitrile.<sup>33</sup> The emission quantum yields of the powdered samples were determined by an Absolute Photo-Luminescence Quantum Yield Measurement System (Hamamatsu Photonics, C9920-03), which comprised an excitation Xenon light source (the excitation wavelength was set at 380 nm), an integrating sphere, and a red-sensitive multichannel photodetector (Hamamatsu Photonics, PMA-12).

### Synthesis

#### General procedure for the synthesis of *trans*-[ $\text{Ru}(\text{TBP})_4(\text{VB})_2$ ], where Q = S (**1**) or Q = Se (**2**)

Corresponding complex *trans*-[ $\text{Ru}(\text{TBP})_4(\text{OH})_2$ ] (0.20 mmol) was dissolved in 30 ml of chlorobenzene. 4-Vinyl benzoic acid (400 mg, 2.70 mmol) was added to the solution. The reaction mixture was heated at 90 °C for 48 hours. The solvent was removed under reduced pressure. The obtained solid was washed 3 times with diethyl ether (30 ml) in an ultrasound bath and separated by centrifugation. The product as a fine powder was collected and dried in a desiccator.

Compound **1**: isolated as a yellow/orange powder, 424 mg, 96%. Elemental analysis (%): Found N 2.5, C 29.0, H 3.1; Calculated for C<sub>29</sub>H<sub>27</sub>N<sub>2</sub>O<sub>4</sub>: N 2.5, C 29.4, H 3.0;  $\delta$ : 9.39 (8H, m,

4\*H<sup>ortho</sup> pyridine), 8.12 (4H, m, 2\*H<sup>2</sup> vinyl benzoate), 7.39 (4H, m, 2\*H<sup>3</sup> vinyl benzoate), 7.21 (8H, m, 4\*H<sup>meta</sup> pyridine), 6.75 (2H, dd, J = 10.6, 7.0 Hz, 2\*CH), 5.79 (2H, d, J = 17.5Hz, 2\*CHH), 5.26 (2H, d, J = 11.1 Hz, 2\*CHH), 1.27 (36H, s, 12\*);  $\nu$ : 30.22, 35.28, 114.5, 121.8, 126.1, 130.3, 134.1, 136.9, 139.4, 160.9, 164.4, 174.2. FTIR (cm<sup>-1</sup>): 2962s, 2926m, 2867w, 1637s, 1616s, 1560w, 1496m, 1458w, 1417m, 1383w, 1365m, 1314s, 1299s, 1227m, 1174m, 1129m, 1065m, 1025m 911w, 862w, 843w, 830m, 786w, 767w, 748w, 716w. ESI-MS (+): Found for [(TBP)<sub>4</sub>(VB)]<sup>+</sup> 2061.6, Calc. 2061.7; Found for Na[(TBP)<sub>3</sub>(VB)<sub>2</sub>]<sup>+</sup> 2095.6, Calc. 2096.7; Found for [Na-1]<sup>+</sup> 2231.6, Calc. 2231.8. UV-Vis ( $\epsilon$ , M<sup>-1</sup>cm<sup>-1</sup>) = 239 (sh, 5.4·10<sup>4</sup>), 268 (5.7·10<sup>4</sup>).

Compound **2**: isolated as a yellow/orange powder, 475 mg, 92%. Elemental analysis (%): Found: N 2.2, C 25.4, H 2.7; Calculated for : N 2.2, C 25.1, H 2.6;  $\nu$ : 9.65 (8H, m, 4\*H<sup>ortho</sup> pyridine), 8.09 (4H, m, 2\*H<sup>2</sup> vinyl benzoate), 7.49 (4H, m, 2\*H<sup>3</sup> vinyl benzoate), 7.09 (8H, m, 4\*H<sup>meta</sup> pyridine), 6.75 (2H, dd, J = 10.7, 6.6 Hz, 2\*CH), 5.79 (2H, d, J = 17.4Hz, 2\*CHH), 5.26 (2H, d, J = 10.6 Hz, 2\*CHH), 1.26 (36H, s, 12\*);  $\nu$ : 30.26, 35.26, 114.3, 122.0, 125.5, 130.1, 135.0, 137.0, 139.2, 160.9, 164.4, 172.8. FTIR (cm<sup>-1</sup>): 2963s, 2926m, 2868w, 1636s, 1615s, 1560w, 1496m, 1459w, 1417m, 1383w, 1365m, 1314s, 1298s, 1227m, 1174m, 1129m, 1065m, 1025m, 1016w, 909w, 862w, 843w, 830m, 787w, 766w, 748w, 715w. ESI-MS (+): Found for [(TBP)<sub>4</sub>(VB)]<sup>+</sup> 2437.1, Calc. 2436.9; Na[(TBP)<sub>3</sub>(VB)<sub>2</sub>]<sup>+</sup> 2471.6, Calc. 2471.8; Found for [Na-2]<sup>+</sup> 2471.6, Calc. 2471.8; Found for [Na-2]<sup>+</sup> 2607.2 Calc. 2607.0. UV-Vis ( $\epsilon$ , M<sup>-1</sup>cm<sup>-1</sup>) = 236 (2.4·10<sup>5</sup>), 268 (2.9·10<sup>5</sup>).

### General procedure for co-polymerisation of **1** and **2** with methyl methacrylate, styrene and *N*-vinylcarbazole

Test tubes were charged with chlorobenzene, in which monomer (0.01 v/v MMA, or 0.01 v/v styrene or 0.01 w/v *N*-vinylcarbazole relative to the solvent) and either complex **1** or **2** (0.005-0.10 w/v relative to monomer in the cases of MMA and styrene or 0.005-0.10 w/w in the case of *N*-vinylcarbazole) were fully dissolved by ultrasonication. AIBN (1 mol% in respect to the organic monomer) was added to the reaction mixture. The tubes were sealed with a rubber septum and degassed by purging of nitrogen for 30 minutes. The polymerisation reactions took place for 18 h (PMMA), 24 h (PS) or 72 h (PVK) at 70 °C. Finally, chlorobenzene was evaporated and the polymer products were dissolved in 10 ml of toluene and precipitated in excess of methanol. All polymers were additionally purified by dialysis in toluene. Several compositions of the hybrid materials *n*<sup>x</sup>@*PM* were obtained, where *n* is either compound **1** or **2**, *x* is the quantity of the cluster complex (mg) used per 1 ml or 1 g of the monomer, and *PM* is either PMMA, PS, or PVK (Table 1). For the sake of comparison the free radical copolymerisation of the styrene, MMA and *N*-vinylcarbazole were performed under the same conditions in the absence of the cluster complexes.

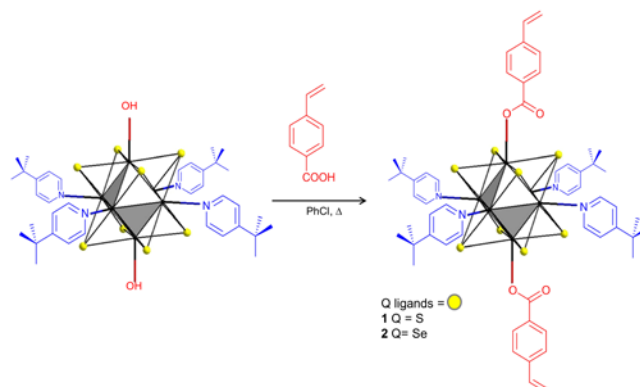
### PLED Fabrication and Electroluminescence Measurements

Light-emitting devices were fabricated on ITO-coated glass substrates (100 nm, Xin Yan Technology Ltd). The substrates were cleaned by ultrasonic bath in acetone, propan-2-ol, 2% Helmanex solution, and deionised water. PEDOT:PSS (Heraeus Clevios™ P VP AI 4083) films were spin coated at 2000 RPM. The active layers were spin-coated onto PEDOT:PSS layers from dichlorobenzene, which consisted of a PVK-based hybrid material (**1**<sup>10</sup>@PVK) in combination with PBD and TPD. Two compositions of active layers were examined: A) 5 mg/ml of **1**<sup>10</sup>@PVK, 2.5 mg/ml of PBD and 1 mg/ml of TPD and B) 4 mg/ml of copolymerized cluster **1**<sup>10</sup>@PVK, 2 mg/ml of PBD and 0.8 mg/ml of TPD (referred to later as compositions **A** and **B**, respectively). The prepared films were dried in air at 120 °C before further processing and characterisation. The thicknesses of the active layer films were ~40 nm as determined by stylus profilometry (Dektak XT). A 0.7 nm thick layer of LiF was deposited by evaporation onto the active layer. Finally, 100 nm thick Al cathodes were prepared by evaporation. The electrical characteristics were measured by a Keithley 2401 SMU. The electroluminescence spectra were recorded with a SpectraScan 655. The emission was found to be uniform throughout the area of each device.

## RESULTS AND DISCUSSION

### Synthesis and characterisation of *trans*-[(TBP)<sub>4</sub>(VB)<sub>2</sub>] cluster complexes

Complexes *trans*-[(TBP)<sub>4</sub>(VB)<sub>2</sub>] (Q = S (**1**), Se (**2**)) were obtained according to the recently developed approach, in which the neutral complexes *trans*-[(TBP)<sub>4</sub>(OH)<sub>2</sub>] were treated by an excess of a relevant carboxylic acid to allow the metathesis between the two hydroxyl-groups of the cluster complex and the corresponding carboxylate anions.<sup>14, 32</sup> Specifically, heating the solutions containing *trans*-[(TBP)<sub>4</sub>(OH)<sub>2</sub>] (Q = S or Se) with an excess amount of 4-vinylbenzoic acid in chlorobenzene for 2 days (Scheme 1) gave the neutral complexes **1** and **2**, respectively, with yields of over 90% after precipitation in, and washing by, diethyl ether.



**Scheme 1.** Synthesis of cluster precursors *trans*-[(TBP)<sub>4</sub>(VB)<sub>2</sub>] (Q = S (**1**), Se (**2**)). The central octahedron represents the cluster whilst the Q ligands are denoted by the yellow spheres.

As expected, upon coordination of 4-vinylbenzoic acid the signals from the aromatic ring protons are shifted to

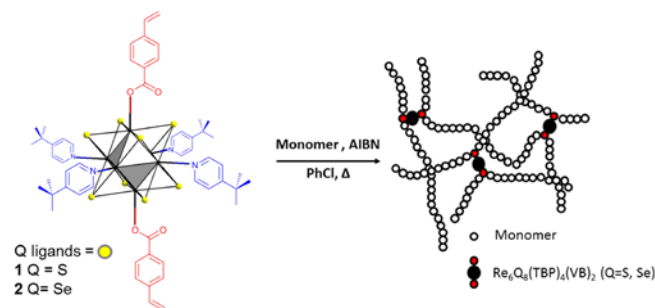
lower field in the  $^1\text{H}$  NMR spectra in comparison with those from the free acid.  $^1\text{H}$  NMR also showed that during the reaction some *trans* to *cis* isomerisation occurred producing less than 5 % of the *cis*-isomer (Figure S1 in Electronic Supplementary Information). Such isomerisation during substitution reactions of the OH groups in *trans*- $[\{\text{TBP}\}_4(\text{OH})_2]$  with carboxylic acid derivatives is fully consistent with previous reports.<sup>14, 32</sup> The isomers were not separated due to the very low percentage of the *cis*-isomer.

Elemental analysis data of **1** and **2** were in good agreement with the chemical formula compositions proposed above and are supported by NMR and ESI-MS analysis. In the positive area of the mass-spectra ionic peaks that correspond to  $\text{Na}[\{\text{TBP}\}_4(\text{VB})_2]^+$  adducts and their dissociation daughter species  $\text{Na}[\{\text{TBP}\}_3(\text{VB})_2]^+$  and  $[\{\text{TBP}\}_4(\text{VB})]^+$  were observed. Complexes **1** and **2** were further characterised by FTIR spectroscopy. FTIR spectra of **1** and **2** have several changes in comparison with the starting cluster complexes and the acid. Specifically, two readily distinguishable bands appeared at 1314 and 1299  $\text{cm}^{-1}$ . These bands correspond to  $\nu(\text{COO})$  in the carboxylate groups present in **1** and **2**. These bands are slightly shifted from those of 4-vinylbenzoic acid (1334 and 1298  $\text{cm}^{-1}$ ), while the stretching  $\text{C}=\text{O}$  vibration of the free acid (1684  $\text{cm}^{-1}$ ) disappeared. At the same time a  $\nu(\text{C}=\text{O})$  vibration is not observed as a defined band in the infrared spectra of the products as it most likely coincides with the band at 1615  $\text{cm}^{-1}$  that is present in the starting complexes  $[\{\text{TBP}\}_4(\text{OH})_2]$ , which is associated with the ring stretching vibrations for *tert*-butylpyridine (Figure S2). Notable, among octahedral cluster complexes of Mo, W and Re, only a handful of examples of complexes with aromatic carboxylic acids are described in the literature.<sup>2, 32, 34</sup> These include the earlier work that describes the related compounds  $[\{\text{TBP}\}_4(\text{L})_2]$  (where L is 3,4,5-trimethoxybenzoic acid or its derivative, *i.e.* gallate-like derivatives),<sup>32</sup> in which a very similar vibration band around 1615  $\text{cm}^{-1}$  was assigned to  $\nu(\text{C}=\text{O})$ , shifted as a result of coordination to the cluster complex. However, the overlap of these vibrations with those from the aromatic ring stretching was not mentioned in this report. In another report, describing complexes  $(\text{L})_2[\{\text{TBP}\}_4(\text{OH})_2]$  with similar L carboxylate anions,<sup>21</sup> infrared spectroscopy showed  $\nu(\text{C}=\text{O})$  to be shifted from 1684  $\text{cm}^{-1}$  to 1630  $\text{cm}^{-1}$ . This again demonstrates the general tendency for  $\nu(\text{C}=\text{O})$  from coordinated carboxylate ligands to occur at lower wave numbers and is therefore consistent with the assumption made for compounds **1** and **2**.

### Preparation of the “ cluster – organic polymer” hybrid materials

In contrast to the polymerisable complex  $[\{\text{TBP}\}_4(\text{MAC})_2]$  reported previously, compounds **1** and **2** have reasonably good solubility, of up to 15 mg/ml in chlorinated solvents, and therefore they can be copolymerised easily with organic monomers using solution-based techniques. This also allows copolymers with much higher rhenium cluster content in the polymer to be obtained than was possible for the previously developed rhenium cluster

complex. Accordingly, we assessed the application of **1** and **2** for synthesis of soluble photoluminescent polymers based on PMMA, PS and PVK and studied the photophysical properties of the latter. Specifically, several samples of polymers with various cluster contents (Table 1) were obtained by free radical copolymerisation reactions of **1** or **2** (0.005–0.10 w/v of MMA or styrene; 0.005–0.10 w/w N-PVK) with the corresponding monomers dissolved in a 10-fold excess of chlorobenzene and initiated by AIBN (1 mol% of the monomer) (Scheme 2). Chlorobenzene was chosen as the reaction solvent not only due to its high boiling temperature and for the ability to dissolve **1** and **2**, but also because of its non-coordinating nature, which meant that complexes **1** and **2** were not likely to be degraded during the polymerisation reaction. The maximum amount of the cluster complexes was limited to 0.10 (w/v of MMA or styrene, w/w PVK) as polymeric products formed which contain higher cluster-loading had low solubilities due to the inherent higher levels of cross-linking. The optimal time of reaction at 70 °C was determined to be 18 h for PMMA, 24 h for PS and 72 h for PVK systems, as after these reaction times both GPC and NMR analysis showed only trace amounts of residual monomer, *i.e.* full conversion has occurred. The polymer products were obtained by evaporation and dissolved in toluene to give clear, coloured solutions. Subsequent isolation was effected by precipitation in methanol and additional purification was accomplished by dialysis in toluene (in the case of PMMA and PS-based polymers).



**Scheme 2** Synthesis of hybrid polymeric materials

To show that the 4-vinyl benzoate ligands do indeed take part in the copolymerisation reaction a control experiment was performed, which employed 5wt % of  $[\{\text{TBP}\}_4(\text{OH})_2]$  instead of **1** in a test copolymerisation reaction with MMA. The product of this reaction after being dissolved did not give a clear solution in either toluene, or THF and the  $^1\text{H}$  NMR spectrum of the isolated precipitate was identical to the starting  $[\{\text{TBP}\}_4(\text{OH})_2]$ .

### Characterisation of the hybrid materials

The polymers containing cluster complexes **1** and **2** with the concentrations up to 0.10 (w/v for PMMA and PS based polymers and w/w for PVK) showed good solubility in a variety of organic solvents including those in which the starting cluster compounds are insoluble (*e.g.* THF and toluene). This is a non-direct proof for both the successful copolymerisation of complexes **1** and **2** with the corresponding monomers as well as the fact that the level of crosslinking, inevitably formed due to the dual-functional

nature of the clusters, is not at a significant enough level to produce insoluble, cross-linked polymers.<sup>35, 36</sup> Accordingly, it proved facile to characterise the resultant materials by GPC using THF as an eluent.<sup>35, 36</sup> The GPC data (Table 1 and Figure S3) show that the average molecular weights as well as the profiles of the molecular weight distributions of polymers containing cluster complexes **1** or **2** are close to those determined for the reference samples of PMMA, PS and PVK.

The IR spectra obtained for the pure polymers and hybrid materials were also very similar due to the relatively low molar concentration of the cluster complexes in the samples and the relatively insensitive nature of the technique. In the aromatic region of the <sup>1</sup>H NMR spectra, however, the signals of protons from pyridine coordinated to the cluster complex were clearly evident as was the signal of *tert*-butyl group at 1.19 ppm. Moreover, these signals were stronger in samples with higher loadings of cluster complexes in the polymer samples (Figure S4).

Differential scanning calorimetry (DSC) and thermal gravimetric analysis (TGA) performed on all samples indicate that the introduction of the cluster complexes resulted in only a limited effect on the thermal properties of the materials as well as on the molecular masses ( $M_n$ ) of the polymers. This was apparent as  $M_n$  and  $M_w$  for all cluster-containing samples were found to be close to those detected for the neat reference polymers (Table 1).

**Table 1** Thermal data and molecular masses of copolymer samples  $n^x@PM$  (where  $n$  refers to compound **1** or **2**,  $x$  refers to content of the cluster (mg) per ml (MMA, styrene) or per g (*N*-vinyl carbazole), and  $PM$  to the type of organic polymer) and corresponding neat polymers.

Sample	Mol. Conc. x 10 <sup>3</sup>	$T_g$ , °C	$T_d$ , °C	$M_n$ , kD
<b>PMMA</b>	–	<b>111</b>	<b>278</b>	<b>22.8</b>
<b>1</b> <sup>10</sup> @PMMA	0.5	90	270	24.3
<b>2</b> <sup>10</sup> @PMMA	0.4	110	269	23.8
<b>2</b> <sup>12.5</sup> @PMMA	0.5	127	287	23.7
<b>2</b> <sup>20</sup> @PMMA	0.8	109	267	24.5
<b>2</b> <sup>30</sup> @PMMA	1.2	110	276	23.3
<b>2</b> <sup>40</sup> @PMMA	1.6	110	286	26.4
<b>2</b> <sup>100</sup> @PMMA	4.1	–	260	19.8
<b>PS</b>	–	<b>110</b>	<b>363</b>	<b>11.5</b>
<b>1</b> <sup>5</sup> @PS	0.3	100	367	10.5
<b>1</b> <sup>10</sup> @PS	0.5	104	381	9.5
<b>1</b> <sup>25</sup> @PS	1.3	119	381	11.6
<b>1</b> <sup>100</sup> @PS	5.2	100	390	9.0
<b>2</b> <sup>5</sup> @PS	0.2	96	383	11.7
<b>2</b> <sup>10</sup> @PS	0.4	83	378	11.8
<b>2</b> <sup>25</sup> @PS	1.1	80	382	10.9
<b>2</b> <sup>100</sup> @PS	4.4	107	389	8.9
<b>PVK</b>	–	<b>222</b>	<b>410</b>	<b>33.4</b>
<b>1</b> <sup>5</sup> @PVK	0.4	227	380	26.1
<b>1</b> <sup>10</sup> @PVK	0.9	229	402	29.4
<b>1</b> <sup>20</sup> @PVK	1.7	227	406	30.3
<b>1</b> <sup>100</sup> @PVK	8.7	235	390	25.3
<b>2</b> <sup>5</sup> @PVK	0.4	233	406	28.2
<b>2</b> <sup>10</sup> @PVK	0.7	230	415	28.6
<b>2</b> <sup>20</sup> @PVK	1.5	237	393	28.8

### Characterisation of photophysical properties

The emission spectra of cluster complexes **1** and **2** in the solid state and in dichloromethane solutions are shown in Figure 1, whilst the emission maximum wavelengths ( $\lambda_{em}$ ), quantum yields ( $\Phi$ ), and lifetimes ( $\tau$ ) are summarised in Table 2. Luminescence of compounds **1** and **2** was studied in the solid state and in both aerated and deaerated dichloromethane solutions. The profiles of the emission spectra of the aerated and deaerated solutions for each

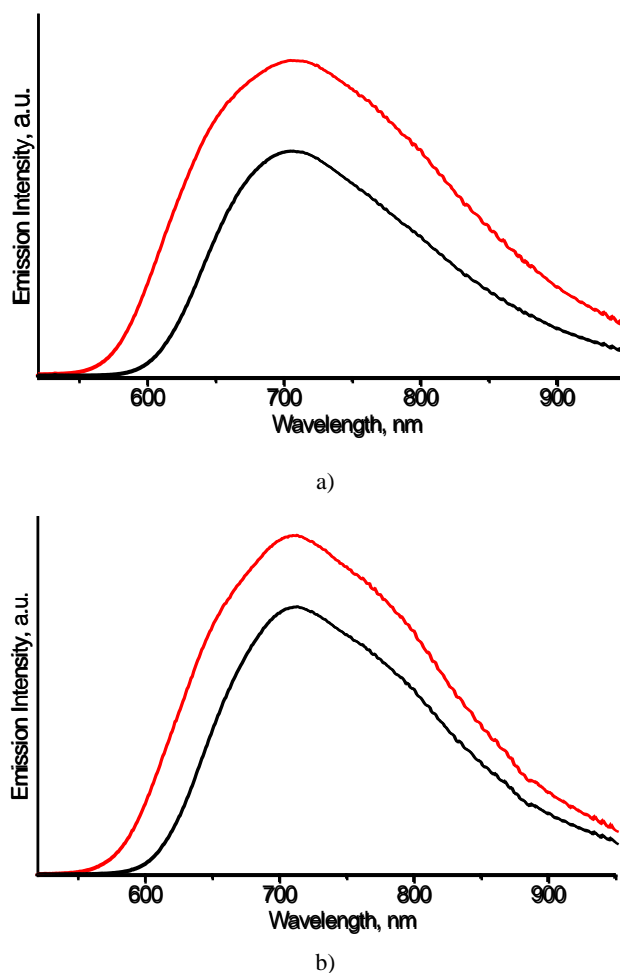


**Figure 1** Emission spectra of powdered samples (a) and deaerated dichloromethane solutions (b) of **1** (black line) and **2** (red line).

sample are identical, however the deaerated solutions are characterised by higher quantum yields and longer lifetimes than those observed for the aerated system (Table 2). This difference is explained readily by the fact that the long-lived luminescence of hexanuclear cluster complexes is well known to be quenched efficiently by oxygen.<sup>3, 4, 6, 7, 15, 37-40</sup> Altogether, the observed photophysical parameters of **1** and **2** are in good accord with other complexes based on the { $\text{Re}^3\text{O}_2$ }<sup>2+</sup> cluster core in various organic solvents.<sup>7, 14-17, 41-43</sup>

To enable the rational development of rhenium cluster-containing materials it is pivotal to understand the impact that binding of the cluster by the polymer matrix (in this particular case co-polymerisation of the cluster's outer lig-

ands with organic monomers to obtain the final polymer) has on the photophysical properties of the cluster units.

Our study shows that powdered samples of the hybrid materials (PMMA, PS and PVK) display a long-lived emission in the region from 550 to more than 950 nm (Table 2 and Figure S5) associated with the phosphorescence of the copolymerised cluster complexes **1** or **2**. This observation signifies that, regardless of monomer, during the polymerisation reaction the cluster complexes retain fully their photoluminescent properties and their chemical integrity, *i.e.* no significant change in chemical environment around the cluster cores occurs during the process. This is in a good agreement with the proposed reaction scheme. At the same time, the emission quantum yields as well as the excited state life times for the PMMA and PS hybrid materials (containing either **1** or **2**) are higher than those found for aerated dichloromethane solutions and powdered samples of the complexes and close to those found for deaerated solutions of **1** and **2**. This observation indicates clearly the strong shielding effect that the PMMA and PS polymer matrices confer against oxygen quenching of the photoluminescence emission associated with the  $\{ \}^{2+}$  cluster core.

**Table 2** Spectroscopic and photophysical data of **1** and **2** as well as copolymer samples  $n^x@PM$  (where  $n$  refers to compound **1** or **2**,  $x$  refers to content of the cluster (mg) per ml (MMA, styrene) or per g (*N*-vinyl carbazole), and  $PM$  to the type of organic polymer).

Sample	$\lambda_{max}$ , nm	$\phi$	$\tau$ , $\mu$ s (Amplitude)
<b>1</b> <sup>a</sup>	~710	0.02 <sup>c</sup>	4.4
<b>1</b> <sup>b</sup>	~710	0.08 <sup>c</sup>	15.8
<b>1</b> (powder)	705	0.05 <sup>d</sup>	$\tau_1 = 9.7$ (0.3); $\tau_2 = 2.5$ (0.7)
<b>2</b> <sup>a</sup>	~710	0.05 <sup>c</sup>	8.1
<b>2</b> <sup>b</sup>	~710	0.10 <sup>c</sup>	15.9
<b>2</b> (powder)	~705	0.07 <sup>d</sup>	$\tau_1 = 9.7$ (0.6); $\tau_2 = 2.9$ (0.4)
<b>1</b> <sup>10</sup> @PMMA	~710	0.06 <sup>d</sup>	$\tau_1 = 16.4$ (0.5); $\tau_2 = 8.8$ (0.5)
<b>2</b> <sup>10</sup> @PMMA	~710	0.07 <sup>d</sup>	$\tau_1 = 14.4$ (0.7); $\tau_2 = 5.0$ (0.3)
<b>2</b> <sup>12.5</sup> @PMMA	~710	0.08 <sup>d</sup>	$\tau_1 = 14.1$ (0.6); $\tau_2 = 5.7$ (0.4)
<b>2</b> <sup>20</sup> @PMMA	~710	0.08 <sup>d</sup>	$\tau_1 = 14.3$ (0.6); $\tau_2 = 5.5$ (0.4)
<b>2</b> <sup>30</sup> @PMMA	~710	0.08 <sup>d</sup>	$\tau_1 = 13.9$ (0.6); $\tau_2 = 4.5$ (0.4)
<b>2</b> <sup>40</sup> @PMMA	~710	0.07 <sup>d</sup>	$\tau_1 = 14.3$ (0.6); $\tau_2 = 5.7$ (0.4)
<b>2</b> <sup>100</sup> @PMMA	~710	0.07 <sup>d</sup>	$\tau_1 = 14.3$ (0.6); $\tau_2 = 5.6$ (0.4)
<b>1</b> <sup>25</sup> @PS	~710	0.07 <sup>d</sup>	$\tau_1 = 16.5$ (0.3); $\tau_2 = 8.1$ (0.7)
<b>1</b> <sup>100</sup> @PS	~710	0.07 <sup>d</sup>	$\tau_1 = 14.7$ (0.3); $\tau_2 = 7.1$ (0.7)
<b>2</b> <sup>5</sup> @PS	~710	0.08 <sup>d</sup>	$\tau_1 = 13.0$ (0.4); $\tau_2 = 6.2$ (0.6)
<b>2</b> <sup>10</sup> @PS	~710	0.09 <sup>d</sup>	$\tau_1 = 13.9$ (0.4); $\tau_2 = 5.6$ (0.6)
<b>2</b> <sup>25</sup> @PS	~710	0.09 <sup>d</sup>	$\tau_1 = 12.6$ (0.4); $\tau_2 = 5.8$ (0.6)
<b>2</b> <sup>100</sup> @PS	~710	0.07 <sup>d</sup>	$\tau_1 = 11.2$ (0.4); $\tau_2 = 4.8$ (0.6)
<b>1</b> <sup>0.5</sup> @PVK	~420, ~710	0.03 <sup>e</sup>	–
<b>1</b> <sup>1</sup> @PVK	~420, ~710	0.03 <sup>e</sup>	–
<b>1</b> <sup>2</sup> @PVK	~420, ~710	0.04 <sup>e</sup>	–
<b>1</b> <sup>10</sup> @PVK	~420, ~710	0.04 <sup>e</sup>	$\tau_1 = 7.8$ (0.02); $\tau_2 = 1.5$ (0.01); $\tau_3 = 0.094$ (0.97)
<b>2</b> <sup>0.5</sup> @PVK	~420, ~710	0.04 <sup>e</sup>	–
<b>2</b> <sup>1</sup> @PVK	~420, ~710	0.04 <sup>e</sup>	–
<b>2</b> <sup>2</sup> @PVK	420,	0.05 <sup>e</sup>	$\tau_1 = 8.3$ (0.02); $\tau_2 = 1.7$ (0.01);

	~710		$\tau_3 = 0.10$ (0.970)
<b>2</b> <sup>10</sup> @PVK	~420,	0.04 <sup>e</sup>	$\tau_1 = 9.2$ (0.02); $\tau_2 = 1.9$ (0.01)
	~710		$\tau_3 = 0.10$ (0.97)
<b>PVK</b>	~420	–	–

<sup>a</sup> Aerated dichloromethane solution;

<sup>b</sup> Deaerated dichloromethane solution;

<sup>c</sup> Relative quantum yield;

<sup>d</sup> Absolute quantum yield;

<sup>e</sup> Absolute quantum yield calculated for the emission region from 600 to 950 nm.

In the case of the PVK hybrid system two emission maxima have been observed that are associated with the fluorescence of PVK (~420 nm) and the phosphorescence of the cluster units (~710 nm) (Table 2). Moreover, the emission of PVK at  $\lambda_{max} = 420$  nm shows some spectral overlap with the absorption spectra of clusters **1** and **2** (Figure 2). Thus, energy transfer from PVK to either complex would be expected. Indeed, when the cluster complex content in the hybrid PVK material was increased it led to an increase in the intensity ratio of the red emission versus the blue emission, confirming this assumption (Figure 3).

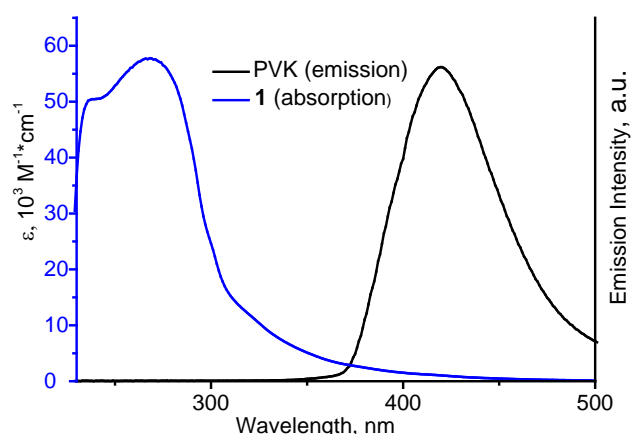


**Figure 2** Absorption spectrum of **1** (dichloromethane solution) and emission spectrum of the neat PVK.

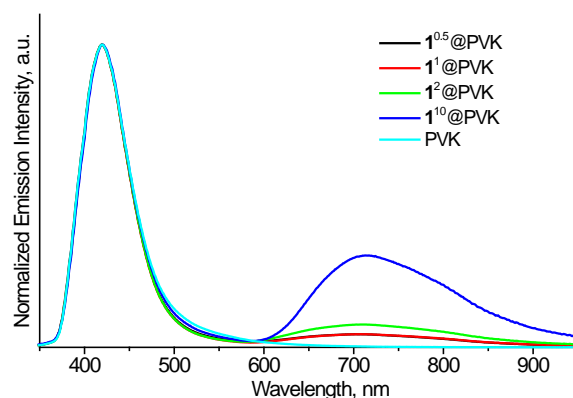


**Figure 3** Emission spectra of the hybrid materials **1** <sup>$x$</sup> @PVK normalised on PVK emission maximum (where  $x$  refers to content of the cluster (mg) per g (*N*-vinyl carbazole)).

Emission decay profiles of aerated and deaerated dichloromethane solutions of **1** and **2** were fitted by single exponential functions while the profiles of the powdered samples of **1** and **2** as well as those obtained from the hybrid materials were fitted to two- or three-exponential decays (Table 2). The  $\tau_2$  components for the solid samples **1**, **2**,  $n^x$ @PMMA and  $n^x$ @PS can be attributed to excitation energy migration and subsequent emission from energy-trap sites, because in the solid state excitation-energy transfer from a cluster to energy-trap sites (such as, for example, surface defects) is likely to proceed efficiently. A short third component  $\tau_3$  calculated from decays of PVK-based materials refers to the fluorescence of PVK itself.

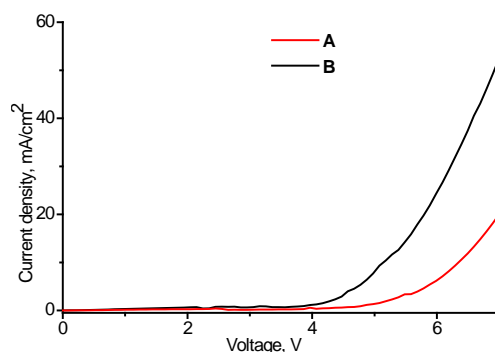
### Characterisation of PLEDs

PVK is well known for its application as an active layer material in PLEDs with the typical working voltage of these devices being around 6-7 V.<sup>44-47</sup> We wished to evaluate the performance of hybrid material **1**<sup>10</sup>@PVK in a PLED. Since the addition of PBD and TPD into the active layer is known to improve electron and hole transport respectively<sup>48-50</sup> and so these materials were also incorporated into the active layer of the PLED. Accordingly a device containing **1**<sup>10</sup>@PVK was constructed and its structure is presented in Figure 4, where either composition **A** or **B** (see Experimental Section) constitutes the active layer. The JV characteristics of both devices (Figure 5) show that the operating voltage of the fabricated devices coincides with those reported for other PVK-based PLEDs. The electroluminescent spectra of the devices recorded at various forward bias show two distinctive peaks of emission associated with the emission of PVK (having a maximum at 465 nm) and a broad emissive signal between ~600 nm and ~800 nm associated with the rhenium cluster unit (Figure 6). Overall emission intensity of the devices was found to be the highest when the voltage applied was 8-9V. When a voltage higher than 11V was applied to the device it caused degradation of the device and a concomitant decline in electroluminescence intensity. Our data also show that the relative intensities of the blue (PVK host) and red (rhenium cluster) peaks change with increased voltages. This observation we ascribe to the fact that at lower voltage, emission from PVK dominates over emission of the cluster complex while at higher voltages the situation is reversed and cluster complex emission predominates. Such behaviour results in overall tuning of the device colour with a reversible voltage-dependent shift from blue to red (Figure 7). Altogether these findings may signify that both subsystems behave independently and energy transfer from blue emitting PVK to { } clusters is absent or not significant. Our observations rather show that excitons form in both subsystems independently.

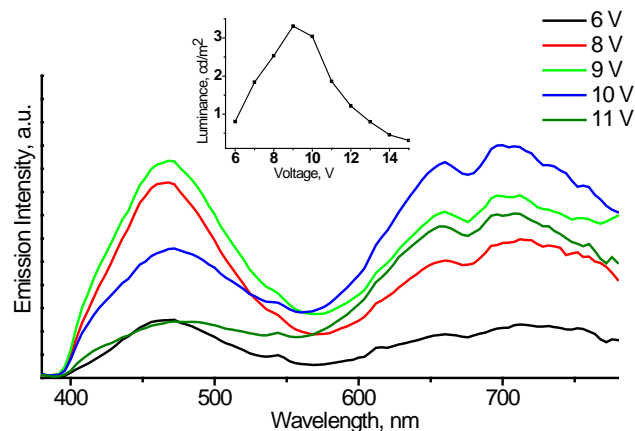


**Figure 4** PLED device stack, ITO: Indium-Tin Oxide.

The overall performances of the two devices are currently quite poor when judged against the well-established PVK/Ir( ) systems.<sup>51</sup> This is likely due to the rhenium cluster concentration being insufficient, resulting in a mixed emission from both the PVK and the rhenium clusters. To improve device performance will demand more detailed studies on the electronic structure of the  $\{(TBP)_4(VB)_2\}$  and further device optimisation. Avenues we are now keen to explore in this direction are to i) work with a new host material(s) with more appropriate HOMO and LUMO levels; ii) alter the concentration of the rhenium clusters, possibly in conjunction with the use of clusters bearing only one polymerisable group to enable higher cluster concentrations to be achieved without significant levels of cross-linking; iii) vary the overall device structure.



**Figure 5** The I-V characteristics of PLEDs with active layers **A** and **B**.



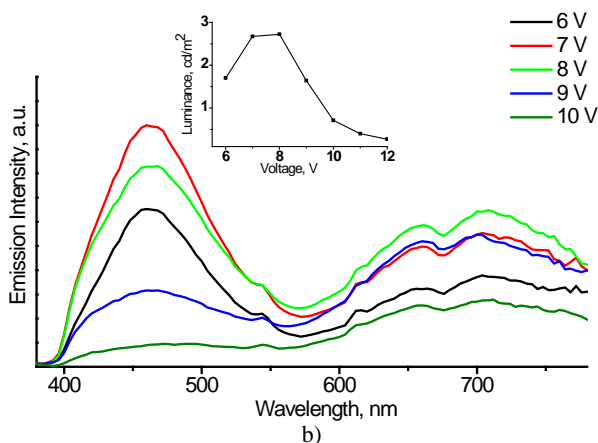


**Figure 6** Electroluminescence spectra of PLEDs with active layer 1 (a) and 2 (b). Inset: Luminance/Voltage characteristics.

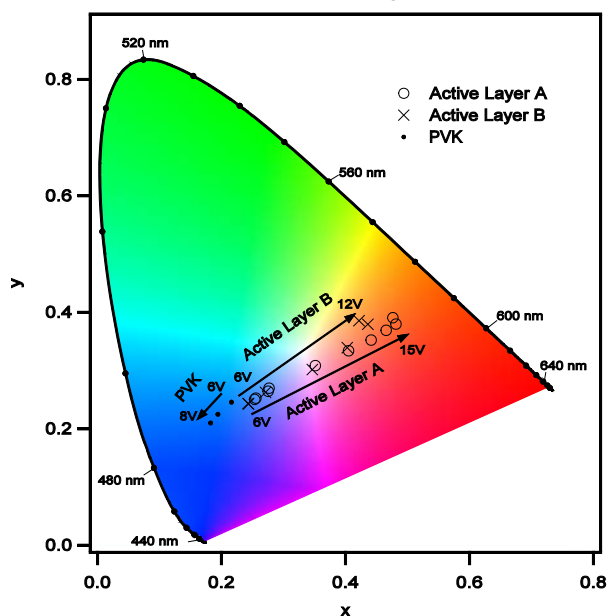


**Figure 7** The colour of the emission of PLEDs with active layer A and B on the CIE colour diagram. The reference PVK is an identical device fabricated from neat PVK (A and B refer to active layers comprising A: 5 mg/ml of  $\text{I}^{10}$ @PVK, 2.5 mg/ml of PBD and 1 mg/ml of TPD and B: 4 mg/ml of copolymerized cluster  $\text{I}^{10}$ @PVK, 2 mg/ml of PBD and 0.8 mg/ml of TPD).

## CONCLUSIONS

In summary, we have developed a facile synthesis of a new type of polymerisable { }-based cluster complexes. These materials have been fully characterised and give analytical data that is entirely consistent with previously described complexes with related structures. The ready solubility of these new polymerisable entities has enabled their successful incorporation into polymers using a widely employed solution-based free radical polymerisation methodology. The approach we have developed is generally applicable and should enable cluster complexes to be incorporated into a host of other polymer types including those key for photo- and electroluminescence applications. Moreover, we have shown that these new polymerisable cluster complexes are stable to free polymerisation reaction conditions

and retain their photoluminescent properties in the resultant hybrid materials.

Finally, we have been able to incorporate the hybrid polymer cluster materials into prototype LED devices. Whilst still requiring optimisation, by developing these rhenium cluster-based PLED devices we have provided the first direct evidence of the electroluminescent properties of rhenium clusters and indeed, to the best of our knowledge, of any member of the family of 24-electron hexanuclear cluster complexes of molybdenum, tungsten or rhenium.

## ACKNOWLEDGMENT

This work was supported by the joint international exchange grant of the Russian Foundation for Basic Research (Grant No. 14-03-92612) and the Royal Society (Grant No. IE140281) and by a Marie Curie Inter-European Fellowship (Grant No. 327440). Also K. A. Brylev thanks the Japan Society for the Promotion of Science (JSPS) for a Post Doctoral Fellowship for Foreign Researchers.

## NOTES AND REFERENCES

<sup>a</sup> Chemical Engineering and Applied Chemistry, Aston University, Aston Triangle, Birmingham, B4 7ET, UK; Fax: +44 (0)121 204 3679; Tel:+44 (0)121 204 3425; E-mail:

a.j.sutherland@aston.ac.uk

<sup>b</sup> Nikolaev Institute of Inorganic Chemistry SB RAS, 3 Acad. Lavrentiev Ave., 630090 Novosibirsk, Russia; Fax: +7(383) 330-94-89; Tel: +7(383) 330-92-53; E-mail: kbrylev@gmail.com

<sup>c</sup> Novosibirsk State University, 2 Pirogova Str., 630090 Novosibirsk, Russia

<sup>d</sup> Department of Soft Matter Physics, Johannes-Kepler University, Altenbergerstr. 69, Linz, A-4040, Austria

<sup>e</sup> Linz Institute for Organic Solar Cells (LIOS), Physical Chemistry, Johannes Kepler University, Linz 4040, Austria

<sup>f</sup> Department of Chemistry, Faculty of Science, Hokkaido University, 060-0810 Sapporo, Japan

† Electronic supplementary information (ESI) available: NMR, FTIR, emission spectra and emission decay profiles, TGA, DSC and GPC analyses, and photographic images of PLEDs. See DOI: 10.1039/xxxxxxx.

1. L. F. Szczepura, K. A. Ketcham, B. A. Ooro, J. A. Edwards, J. N. Templeton, D. L. Cedeno and A. J. Jircitano, *Inorg. Chem.*, 2008, **47**, 7271-7278.
2. Y. Molard, F. Dorson, V. Circu, T. Roisnel, F. Artzner and S. Cordier, *Angew. Chem., Int. Ed.*, 2010, **49**, 3351-3355.
3. M. N. Sokolov, M. A. Mihailov, E. V. Peresytkina, K. A. Brylev, N. Kitamura and V. P. Fedin, *Dalton Trans.*, 2011, **40**, 6375-6377.
4. K. Kirakci, P. Kubat, J. Langmaier, T. Polivka, M. Fuciman, K. Fejfarova and K. Lang, *Dalton Trans.*, 2013, **42**, 7224-7232.
5. Y. Molard, C. Labbe, J. Cardin and S. Cordier, *Adv. Funct. Mater.*, 2013, **23**, 4821-4825.
6. M. N. Sokolov, M. A. Mikhailov, K. A. Brylev, A. V. Virovets, C. Vicent, N. B. Kompankov, N. Kitamura and V. P. Fedin, *Inorg. Chem.*, 2013, **52**, 12477-12481.

7. T. G. Gray, C. M. Rudzinski, E. E. Meyer, R. H. Holm and D. G. Nocera, *J. Am. Chem. Soc.*, 2003, **125**, 4755-4770.
8. Y. V. Mironov, K. A. Brylev, M. A. Shestopalov, S. S. Yarovoi, V. E. Fedorov, H. Spies, H.-J. Pietzsch, H. Stephan, G. Geipel, G. Bernhard and W. Kraus, *Inorg. Chim. Acta*, 2006, **359**, 1129-1134.
9. M. A. Shestopalov, Y. V. Mironov, K. A. Brylev, S. G. Kozlova, V. E. Fedorov, H. Spies, H.-J. Pietzsch, H. Stephan, G. Geipel and G. Bernhard, *J. Am. Chem. Soc.*, 2007, **129**, 3714-3721.
10. K. A. Brylev, Y. V. Mironov, S. G. Kozlova, V. E. Fedorov, S.-J. Kim, H.-J. Pietzsch, H. Stephan, A. Ito, S. Ishizaka and N. Kitamura, *Inorg. Chem.*, 2009, **48**, 2309-2315.
11. M. A. Shestopalov, S. Cordier, O. Hernandez, Y. Molard, C. Perrin, A. Perrin, V. E. Fedorov and Y. V. Mironov, *Inorg. Chem.*, 2009, **48**, 1482-1489.
12. K. A. Brylev, Y. V. Mironov, V. E. Fedorov, S.-J. Kim, H.-J. Pietzsch, H. Stephan, A. Ito and N. Kitamura, *Inorg. Chim. Acta*, 2010, **363**, 2686-2691.
13. A. Kahnt, L. P. Heiniger, S. X. Liu, X. Y. Tu, Z. Zheng, A. Hauser, S. Decurtins and D. M. Guldi, *ChemPhysChem*, 2010, **11**, 651-658.
14. Y. Molard, F. Dorson, K. A. Brylev, M. A. Shestopalov, Y. Le Gal, S. Cordier, Y. V. Mironov, N. Kitamura and C. Perrin, *Chem. Eur. J.*, 2010, **16**, 5613-5619.
15. L. F. Szczepura, D. L. Cedeno, D. B. Johnson, R. McDonald, S. A. Knott, K. M. Jeans and J. L. Durham, *Inorg. Chem.*, 2010, **49**, 11386-11394.
16. T. Yoshimura, C. Suo, K. Tsuge, S. Ishizaka, K. Nozaki, Y. Sasaki, N. Kitamura and A. Shinohara, *Inorg. Chem.*, 2010, **49**, 531-540.
17. T. Yoshimura, S. Ishizaka, T. Kashiwa, A. Ito, E. Sakuda, A. Shinohara and N. Kitamura, *Inorg. Chem.*, 2011, **50**, 9918-9920.
18. S. Cordier, Y. Molard, K. A. Brylev, Y. V. Mironov, F. Grasset, B. Fabre and N. G. Naumov, *J. Cluster Sci.*, 2014, DOI: 10.1007/s10876-10014-10734-10870.
19. J.-C. Eloi, L. Chabanne, G. R. Whittell and I. Manners, *Mater. Today*, 2008, **11**, 28-36.
20. M. Kubeil, H. Stephan, H.-J. Pietzsch, G. Geipel, D. Appelhans, B. Voit, J. Hoffmann, B. Brutschy, Y. V. Mironov, K. A. Brylev and V. E. Fedorov, *Chem. Asian J.*, 2010, **5**, 2507-2514.
21. A. S. Mocanu, M. Amela-Cortes, Y. Molard, V. Circu and S. Cordier, *Chem. Commun.*, 2011, **47**, 2056-2058.
22. M. Amela-Cortes, A. Garreau, S. Cordier, E. Faulques, J.-L. Duvail and Y. Molard, *J. Mater. Chem. C*, 2014, **2**, 1545-1552.
23. X. Y. Tu, G. S. Nichol, P. Keng, J. Pyun and Z. P. Zheng, *Macromolecules*, 2012, **45**, 2614-2618.
24. M.-J. Yang and T. Tsutsui, *Jpn. J. Appl. Phys.*, 2000, **39**, L828-L829.
25. X. Yang, D. Neher, D. Hertel and T. K. Daubler, *Adv. Mater.*, 2004, **16**, 161-166.
26. F.-C. Chen, Y. Yang, M. E. Thompson and J. Kido, *Appl. Phys. Lett.*, 2002, **80**, 2308-2310.
27. X. Gong, J. C. Ostrowski, G. C. Bazan, D. Moses and A. J. Heeger, *Appl. Phys. Lett.*, 2002, **81**, 3711-3713.
28. S. D. Kan, X. D. Liu, F. Z. Shen, J. Y. Zhang, Y. G. Ma, G. Zhang, Y. Wang and B. C. Shen, *Adv. Funct. Mater.*, 2003, **13**, 603-608.
29. X. Gong, J. C. Ostrowski, G. C. Bazan, D. Moses, A. J. Heeger, M. S. Liu and A. K. Y. Jen, *Adv. Mater.*, 2003, **15**, 45-49.
30. T. R. Hebner and J. C. Sturm, *Appl. Phys. Lett.*, 1998, **73**, 1775-1777.
31. J. Wang, F. Zhang, B. Liu, Z. Xu, J. Zhang and Y. Wang, *J. Phys. D: Appl. Phys.*, 2013, **46**, 015104.
32. F. Dorson, Y. Molard, S. Cordier, B. Fabre, O. Efremova, D. Rondeau, Y. Mironov, V. Circu, N. Naumov and C. Perrin, *Dalton Trans.*, 2009, 1297-1299.
33. K. Suzuki, A. Kobayashi, S. Kaneko, K. Takehira, T. Yoshihara, H. Ishida, Y. Shiina, S. Oishic and S. Tobita, *Phys. Chem. Chem. Phys.*, 2009, **11**, 9850-9860.
34. N. Prokopuk and D. F. Shriver, *Inorg. Chem.*, 1997, **36**, 5609-5613.
35. A. T. Slark, D. C. Sherrington, A. Titterton and I. K. Martin, *J. Mater. Chem.*, 2003, **13**, 2711-2720.
36. P. A. Costello, I. K. Martin, A. T. Slark, D. C. Sherrington and A. Titterton, *Polymer*, 2002, **43**, 245-254.
37. J. A. Jackson, C. Turro, M. D. Newsham and D. G. Nocera, *J. Phys. Chem.*, 1990, **94**, 4500-4507.
38. L. M. Robinson, H. Lu, J. T. Hupp and D. F. Shriver, *Chem. Mater.*, 1995, **7**, 43-49.
39. J. A. Jackson, M. D. Newsham, C. Worsham and D. G. Nocera, *Chem. Mater.*, 1996, **8**, 558-564.
40. O. A. Efremova, M. A. Shestopalov, N. A. Chirtsova, A. I. Smolentsev, Y. V. Mironov, N. Kitamura, K. A. Brylev and A. J. Sutherland, *Dalton Trans.*, 2014, **43**, 6021-6025.
41. T. Yoshimura, K. Umakoshi, Y. Sasaki, S. Ishizaka, H.-B. Kim and N. Kitamura, *Inorg. Chem.*, 2000, **39**, 1765-1772.
42. T. Yoshimura, Z.-N. Chen, A. Itasaka, M. Abe, Y. Sasaki, S. Ishizaka, N. Kitamura, S. S. Yarovoi, S. F. Solodovnikov and V. E. Fedorov, *Inorg. Chem.*, 2003, **42**, 4857-4863.
43. A. Gandubert, K. A. Brylev, T. T. Nguyen, N. G. Naumov, N. Kitamura, Y. Molard, R. Gautier and S. Cordier, *Z. Anorg. Allg. Chem.*, 2013, **639**, 1756-1762.
44. C. W. Ko and H. C. Lin, *Thin Solid Films*, 2000, **363**, 81-85.
45. Y. Xuan, D. C. Pan, N. Zhao, X. L. Ji and D. G. Ma, *Nanotechnology*, 2006, **17**, 4966-4969.
46. P. D'Angelo, M. Barra, A. CassineSe, M. G. Maglione, P. Vacca, C. Minarini and A. Rubino, *Solid-State Electron.*, 2007, **51**, 123-129.

47. T. M. El-Agez, S. A. Taya, A. A. El Tayyan, M. S. Abdel-Latif and A. Afghjani, *Phys. Rev. Res. Int.*, 2013, **3**, 306-320.
48. M. A. Díaz-García, *J. Polym. Sci. B - Polym. Phys.*, 2003, **41**, 2706-2714.
49. R. Tomova, P. Petrova, R. Stoycheva-Topalova, A. Buroff and J. Pirov, *J. Optoelectron. Adv. Mater.*, 2007, **9**, 501-504.
50. D.-H. Lee, J. S. Choi, H. Chae, C.-H. Chung and S. M. Cho, *Displays*, 2008, **29**, 436-439.
51. *Highly Efficient OLEDs with Phosphorescent Materials*, Ed.: Hartmut Yersin, WILEY-VSH Verlag GmbH, 2008, P.224 and ref therein.

## GRAPHICAL ABSTRACT

Soluble, polymerizable  $Re^{-}$  containing cluster complexes have been developed and polymerised to generate photo/electroluminescent materials, which can be used to construct PLEDs

